

A Blind Image Restoration for Out-of-Focus Blurred Images using Adaptive Inverse Filters

TETSUYA IMAI, RYOJI MIYAKOSHI, and HIRONORI YAMAUCHI
Graduate School of Science and Engineering
Ritsumeikan University
Noji-Higashi 1-1-1, Kusatsu, Shiga, 525-8577
JAPAN

Abstract: This paper presents a new restoration approach to blurred images using inverse filters optimized by a Genetic Algorithm (GA). The proposed approach consists of two procedures. The first is to estimate a degradation level of blurred images based on Discrete Fourier Transform (DFT) and the next is to optimize inverse filters using a Real-coded GA. The degradation level estimation prior to inverse filters optimization enables the adaptive and efficient image restoration according to the blurred level. Experiments on natural images demonstrate that the proposed approach can provide a practical solution for a blind image restoration.

Key-Words: Blind image restoration, Degradation level estimation, Inverse filters, DFT, Real-coded GA.

1 Introduction

Image restoration, which restores an original image from a degraded image by various types of blur and noise, has played a very important role in the field of image processing. In the earlier stage, image restoration began in the area of astronomical imaging. Nowadays, the image restoration target is spreading over various applications, which include the quality improvement for medical imaging, the image enhancement of low-resolution security images, the restoration of deteriorated old movie films, etc [1-3].

The primary approaches of image restoration are classified a direct restoration approach and an iterative restoration approach. The former includes the linear restoration filter, such as a Wiener filter, a general inverse filter, a constrained least squares filter, etc. The latter includes a super-resolution method and a non-linear restoration filter, such as Maximum entropy filter. From the viewpoint of computation time and implementation technique, in general, the direct restoration approach will be more advantageous and practical. In this paper, we propose a new direct restoration approach using optimized pseudo inverse filters by a GA. This is because we consider an image restoration problem as an optimization problem of pseudo inverse filters and utilize GA processing for the efficient optimization of inverse filters due to highly parallel nature of a GA.

A GA, which is a well-known search and optimization algorithm based on genetic evolution process of creatures [4], can search efficiently

sub-optimal solutions from a huge search-space. In the existing studies of GA-based image restoration, a direct coding of 2-dimensional image data into the chromosome has been proposed [5-6]. In case of gray-scale images or large-size images, it will be often unpractical to employ this direct coding method due to its huge computation time. Therefore, we previously proposed a more practical restoration method, which optimizes a restoration inverse filter using a Real-coded GA [7]. However, the proposed method cannot restore the degradation image according to its blurred level due to the fixed degree of the restoration inverse filter. In order to restore adaptively blurred images with various blurring levels, this paper describes a new restoration method, which combines the degradation level estimation with the inverse filter optimization previously proposed.

2 Degradation Model and Restoration System

2.1 Image degradation model

Degradation factors for images are categorized into out-of-focus blur and various kind of aberrations in optical lens system, motion blur due to camera's mistaken operation, noise in image capturing and processing, etc [3]. In conventional image degradation models, a blur and an additive noise are modeled as main degradation factors. However, this paper deals with a narrowed and simplified degradation model,

which confines degradation factors only to out-of-focus blur. The reasons are to clarify the merit of the proposed approach using the simplified model and to make some assumptions for the degradation level estimation. It is assumed that the characteristics of the PSF (Point Spread Function) are known and a presence of an additive noise is not considered. These assumptions are popular in a priori blur identification, which is known as a simple and practical approach in various blur identification approaches [8].

In this paper, out-of-focus blur is expressed by a shift-invariant Gaussian PSF, which is a variable-separable function and is often used in the application of astronomical imaging, X-ray medical imaging, and photography. Therefore, the degradation model can be expressed with a convolution of the Gaussian degradation function $h(x, y)$ into the original image $f(x, y)$.

$$g(x, y) = \sum_{k=-M}^M \sum_{l=-N}^N h(k, l) f(x - k, y - l)$$

$$h(x, y) = K \exp\left(-\frac{x^2 + y^2}{2\sigma^2}\right)$$

$$= \sqrt{K} \exp\left(-\frac{x^2}{2\sigma^2}\right) \sqrt{K} \exp\left(-\frac{y^2}{2\sigma^2}\right)$$

$$= h(x) h(y) \quad (1)$$

where $g(x, y)$ is a degraded image, K is a normalizing constant, σ is a standard deviation indicating the blur severity, M and N are the blur domain spreading over x -direction and y -direction, respectively. Since $h(x, y)$ is variable-separable, it can be separated into $h(x) h(y)$ as shown in Equation (1). In other words, it enables to convert the degradation distributed over 2-dimensional domain into 1-dimensional domain and to handle as the simplified restoration problem. That is, the 2-dimensional FIR filter can be easily realized by independently vertical and horizontal filtering of 1-dimensional FIR filter, which can be provided by the least-squares method.

2.2 Image Restoration Algorithm

The degradation model and its restoration process are indicated in Fig.1. Note that, since the actual restoration is processed on Z coordinates, the original image and the restored image are expressed with $X(Z_1, Z_2)$ and $\hat{X}(Z_1, Z_2)$, respectively.

Since a simplified noiseless degradation model is used as described in section 2.1, the restored image is,

$$\hat{X}(Z_1, Z_2) = F(Z_1, Z_2) H(Z_1, Z_2) X(Z_1, Z_2) \quad (2)$$

The condition for restoring the degraded images is $\hat{X}(Z_1, Z_2) \cong X(Z_1, Z_2)$. In order to satisfy the condition, the following is required, $F(Z_1, Z_2) H(Z_1, Z_2) \cong 1$.

Therefore, an error margin is given in Equation (3).

$$E(Z) = F(Z) H(Z) - 1 \quad (3)$$

An optimal solution (inverse filter f), which will minimize the evaluation function J , can be solved by Equation (4) using the least-squares method.

$$J = e^T e = \|Hf - d\|^2$$

$$= (Hf - d)^T (Hf - d)$$

$$\frac{\partial J}{\partial f} = 2H^T (Hf - d) = 0$$

$$2H^T H f - 2H^T d = 0$$

$$f = (H^T H)^{-1} H^T d = H^+ d \quad (4)$$

where d is a delta matrix and H^+ is a Moore and Penrose inverse matrix. The H^+ will be used in case that H is ill conditioned. Equation (4) means that an inverse filter f can be uniquely determined by the Gaussian degradation function H .

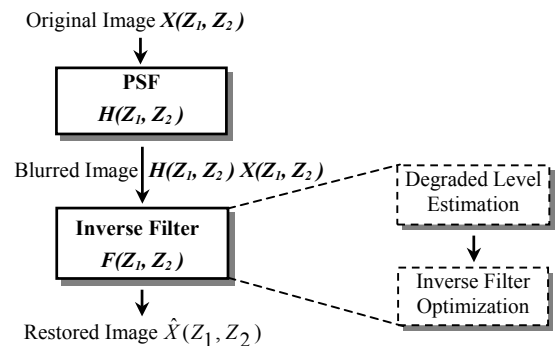


Fig.1 Degradation model and restoration process for images

3 Degradation Level Estimation

This section describes a new method of degradation level estimation based on Discrete Fourier Transform (DFT) spectrum of blurred images, which is a more simple and practical method than methods shown in blur identification approaches [8]. This aims to determine the degree of the restoration inverse filter for narrowing a search-space of GA, because the unclear degradation level produces a huge search-space and prevents an efficient GA search. In other words, the degradation level estimation performs

a kind of pre-processing prior to the optimization of restoration inverse filters as shown in Fig.1.

Fig.2 indicates an example of magnitude spectrums of degradation images in case of applying 2-dimensional DFT operation. Fig.2 demonstrates some changes on magnitude spectrums of 4 blurred images using σ as a degradation level parameter. The horizontal normalized frequency in Fig.2 expresses a period on a diagonal line (that is, $[0, \sqrt{2}\pi]$) in 2-dimensional spectrum space. Note that $[0, 4.5]$ section in the horizontal normalized frequency corresponds to $[0, \sqrt{2}\pi]$ section.

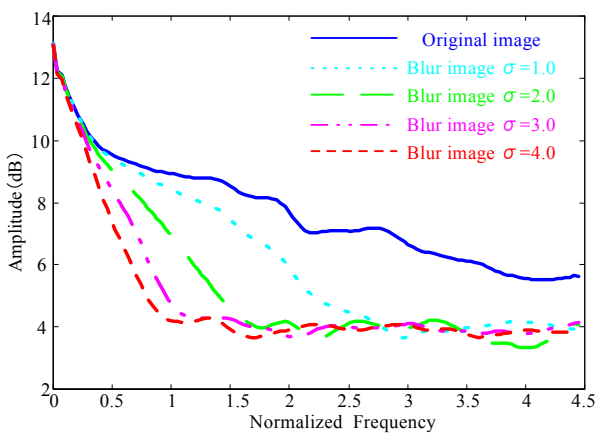


Fig.2 DFT spectrum features on degradation images

When the frequency range in Fig.2 is divided into lower, mid and higher range, magnitude spectrums of degradation images remarkably decrease in mid and higher frequency range with the increase of the degradation. Because mid and higher frequency components will decrease rapidly. After the slope of the decrease curve transiently becomes steep, then the curve maintains nearly constant.

Based on the above feature, it can be considered that the frequency on the intersection point of the decrease slope line and the nearly constant line will reflect the degradation level σ . This leads to the simple and practical estimation method as shown the following steps.

- Step 1: Obtain a 5% higher average spectrum value than the nearly constant line in the higher frequency range.
- Step 2: Determine such a normalized frequency as can give the above average spectrum. (This is called the inflection point frequency.)
- Step 3: Obtain the inflection point frequency for σ of various images.

From this, the statistical relationship between σ and the inflection point frequency will be defined. Here, using sample images “SHIPP” (Wool, Bottles, Bride, and Harbor) employed in experiments in section 5, the statistical relationship will be examined. Since these sample images are all natural images, the relationship between σ and the inflection point frequency expresses almost the same tendency independent of the type of images (Fig.3). Fig.3 indicates that the relationship can be utilized for the degradation level estimation. Consequently, when using the statistical characteristic curve which indicates an average of four characteristic curves, the degradation level will be estimated based on the inflection point frequency.

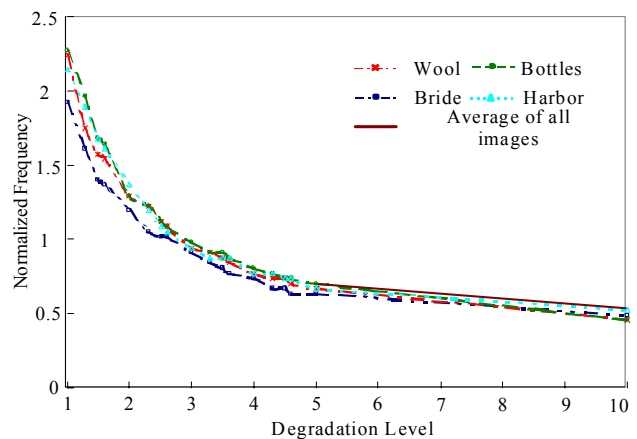


Fig.3 Relationship between degradation level and inflection point frequency

4 Inverse Filter Optimization using Rc-GA

This section describes a design methodology for GA parameters for restoration inverse filters. Note that individuals express restoration inverse filters (2-dimensional FIR filter), chromosomes express real number coefficients of the FIR filter, and genes express real numbers, respectively. Therefore, in order to optimize real numbers, a Real-coded GA (Rc-GA) intended for handling real numbers is employed [9-10].

4.1 Coding of Restoration Inverse Filters

As described in section 2.1, the restoration inverse filter, which is generally expressed by 2-dimensional FIR filter, can be coded into the 1-dimensional FIR filter. The simplified coding enables to shorten the GA computation time. The concept of the 1-dimensional

restoration inverse filter is illustrated in Fig.4. The sign from F0 to Fi-1(i: integer) represents the real number coefficients of restoration inverse filter consisted with i items. And, a standard deviation σ in the Gaussian degradation function represents the parameter indicating the blur severity. These i elements constitutes the restoration inverse filter with i degree. Note that the variable of σ is also adjustable by mutation operation (as described in section 4.5).

The degree of the restoration inverse filter can be set arbitrarily in order to handle the degradation images with various degraded levels. This is because it is required to expand the filter degree according to its degradation levels. From the degradation level estimated in section 3, the filter degree, in which the influence caused by the degradation can be suppressed within 3%, will be selected. In this way, the degree of the restoration inverse filter can be determined based on the degradation level of the blurred images.

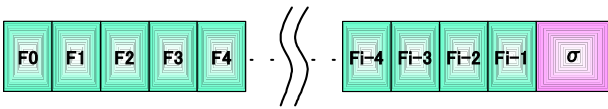


Fig.4 Restoration inverse filter coding

4.2 Initial Population Generation

The generation method for the initial population, which is combined with the degradation level estimation in section 3, is described below.

- Step 1: Estimate the degradation level σ (section 3).
- Step 2: Vary σ minutely at a closer space to the σ estimated above.
- Step 3: Determine a Gaussian degradation function H corresponding to each σ by Equation (1).
- Step 4: Solve an inverse filter f from H by Equation (4).

Consequently, using the above steps, a restoration inverse filter f can be uniquely determined from each σ mentioned above. When an initial population size becomes larger, variety of individuals generally becomes higher and a computation time increases at the same time. Here, with consideration of a tradeoff between a population size and a computation time, 50 individuals (that is, 50 inverse filters) have been selected as the initial population size.

4.3 Fitness Evaluation

In a fitness evaluation, we propose a new method based on DFT spectrums of blurred images, which is

similar to the degradation level estimate proposed in section 3. The reason is as follows. In a conventional fitness evaluation, it is required to restore each degraded image using convolution operations and then to judge quality of restored images. However, without any information on a degradation process and an original image, it will be impossible to judge the quality.

Therefore, we introduce a new evaluation method utilizing two features of DFT spectrums shown in Fig.2: 1) the magnitude spectrum remarkably decreases in mid and higher frequency range. 2) with the increase of the degradation, the starting point of the decrease gradually shifts into the lower frequency range. From the above feature 1), as a fitness for evaluation, we employ the area of the magnitude spectrum at $\left[\frac{\sqrt{2\pi}}{3}, \frac{2\sqrt{2\pi}}{3} \right]$ corresponding to [1.5, 3.0] in the horizontal normalized frequency in Fig.2. The area "A" indicating the fitness can be expressed as follows.

$$A = \int_{\frac{\sqrt{2\pi}}{3}}^{\frac{2\sqrt{2\pi}}{3}} |P(f)| df \quad (5)$$

where $|P(f)|$ is the magnitude spectrum of blurred images. DFT spectrum $P(f)$ can be described as follows.

$$P(k) = \sum_{n=0}^{N-1} p(n) W_N^{kn}, \quad (k=0,1,2,\dots,N-1) \quad (6)$$

$$W_N = \exp\left(-j \frac{2\pi}{N}\right) \quad (N: \text{Integer Number})$$

From the above feature 2), in order to reflect changes of the magnitude spectrum with the increase of the degradation, we allow the target evaluation domain to shift adaptively according to the degradation level. In other words, the target evaluation domain moves gradually from lower and mid range to higher range with the decrease of the degradation. Table 1 summarizes the target evaluation domain, which adaptively shifts according to the estimated degradation level and the number of evolution generations. Note that numerical data in Table 1 indicate average values of normalized frequency acquired by experimental results on natural images including sample images (SHIPP) in section 5. Therefore, numerical data in Table 1 will be generally effective for natural images.

Furthermore, the new method puts a lower evaluation value on individuals, who will not

demonstrate a tendency toward monotonous decrease of the magnitude spectrum from lower range to higher range. Because the superficial evaluation, which focuses attention only on the magnitude spectrum increase in the target evaluation domain, often puts a higher value on individual with an excessively high magnitude spectrum in the domain.

Table 1 Target domain shift for fitness evaluation

Estimated σ	Evolution generation number		
	less than 7	8 – 13	more than 14
less than 1.4	2.4 – 4.1	2.6 – 4.3	2.7 – 4.5
1.4 – 3.0	1.3 – 2.9	1.7 – 3.3	2.4 – 4.1
more than 3.0	1.0 – 2.7	1.3 – 2.9	1.9 – 4.0

Fig.5 indicates, as a typical example, the magnitude spectrum of the blurred and original image on the sample image (Bride) employed in section 5. The magnitude spectrum of the blurred image decreases remarkably in mid and higher range. All sample images in section 5 demonstrate almost the same tendency as shown in Fig.5.

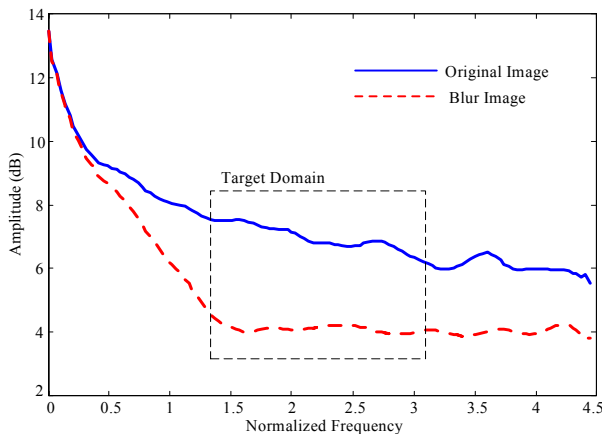


Fig.5 Fourier spectrum example of blurred and original image

4.4 Selection

The selection method employs a dual process combining ranking selection with elitism. The ranking selection is introduced to avoid a premature convergence owing to only elitism and to maintain a variety of individuals.

Using elitism, the best 10% of the current generation will be constantly copied to next generation without any genetic operation. Using ranking selection, individuals will be selected according to the ranking based on their fitness. Then, each ranked individual will consist the rest 60% of the next generation as following rule: 30% of the top ranking will occupy 30%, 40%-60% of the middle range ranking will

occupy 20%, and 80%-90% of the low range ranking will occupy 10% of the next generation. Individuals randomly selected from the current generation will occupy the rest 30% of the next generation. Note that the above rule in ranking selection is based on additional experimental results.

4.5 Genetic Operation

As a genetic operator, an only new mutation operation is employed, which is originally invented for searching the closer space to an optimal solution. A previous proposed method [7] employed two operations, an UNDX (Unimodal Normal Distribution Crossover) operation peculiar to a Rc-GA and a conventional mutation operation. However, since a PSF was assumed to be a Gaussian, this UNDX operation produced many disadvantageous and useless individuals to the Gaussian PSF and resulted in reducing the search efficiency. Consequently, the new mutation operation will be adopted as an only genetic operator.

The procedure of the new mutation operation is to provide random numbers with each σ of the initial population generated in section 4.2, and to regard each σ as a chromosome. Five random number generators generate these random numbers with mutually different accuracy. These five generators will output independently the random number for five digits n_0 to n_4 in Fig.6. The n_0 indicates an integer digit and n_1n_4 indicate first, second, third, and fourth decimal places. Every time five evolution generations progress, the digit required to generate random numbers will be shifted right toward a smaller digit (that is, a digit with higher accuracy). This aims at an exacting search by narrowing a variation range of random search gradually every five generations. In each case, mutation rate is 80%. This is because, for more efficient search of a huge real numbers space, it will be required to minutely search a closer space to an optimal solution.

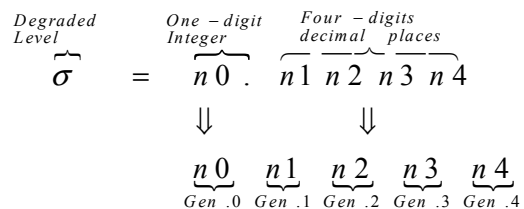


Fig.6 Random number generation for mutation operation

Based on the discussion on the optimization of restoration inverse filters in section 4, the optimization

flow by a Rc-GA is summarized in Fig.7. Surely, as shown in Fig.1, the Rc-GA flow in Fig.7 follows the degradation level estimation described. Here, the condition for the termination is 20 generations, which are selected with consideration of a tradeoff between a restored image quality and a restoration time.

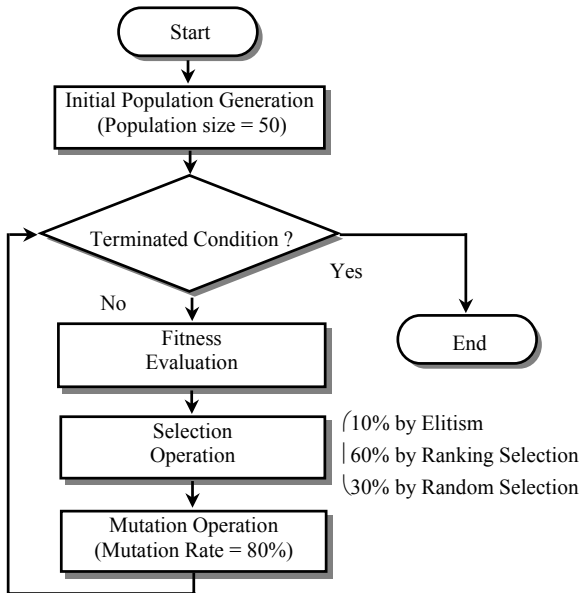


Fig.7 Optimization flow of inverse filter using a Rc-GA

5 Experiments for Image Restoration

Experiments for image restoration employ 4 types of natural images “SHIPP” (Wool, Bottles, Bride, and Harbor) offered by the Institute of Image Electronics Engineers of Japan (IIEEJ) [11]. The features of the SHIPP images will be summarized as follows. Wool is a still life with a wide range of shading, a bottle is a still life with a metallic burnish, a bride is a woman’s portrait with smooth shading, and a harbor is a landscape with many fine edges. These SHIPP images are 256×256 in size and have 256 levels of gray scale.

The experimental results will be evaluated by both a visual inspection and PSNR (Peak Signal to Noise Ratio) of restored images, which provides a basic measure indicating the difference between the original image and the restored image. The restoration results are indicated in Fig.8. Fig.8 (Left) shows blurred images with degradation level $\sigma = 1.0, 1.5, 2.0,$ and $2.5,$ respectively. Fig.8 (Right) shows restoration images for each blurred image.



Blurred image ($\sigma = 1.0$) Restored image
(a) Wool



Blurred image ($\sigma = 1.5$) Restored image
(b) Bottles



Blurred image ($\sigma = 2.0$) Restored image
(c) Bride



Blurred image ($\sigma = 2.5$) Restored image
(d) Harbor

Fig.8 Restoration experiments on natural images

In a visual inspection, Fig.8 demonstrates that, independent of features and blurred level of natural images, 4 types of natural images with out-of-focus

blur are restored with stability. Even in case of sample images with a relatively severe blur (Bride and Harbor), it can be visually confirmed that their edges and details of the restored images (for example, woman's hair and bonnet in Bride, window frames with fine geometrical structures in Harbor) are reasonably well restored. Therefore, in practical situations, the quality of these images will not become significant problems.

Next, in order to evaluate numerically the restoration image quality, PSNR of restoration images will be examined using Equation (7).

$$PSNR = 10 \log_{10} \left(\frac{N \times M \times T^2}{\sum_{i=1}^N \sum_{j=1}^M \|\hat{x}(i, j) - x(i, j)\|^2} \right) \quad (7)$$

where x is an original image and \hat{x} is a restored image, respectively, then $N \times M$ is an image size and T shows {the gray-scale number} -1. For example, in case of 256 levels of gray, $T = 255$.

Table 2 Experimental results (Average)

Blurred Level σ	1.0	1.5	2.0	2.5	3.0
Estimated Blurred Level σ	1.08	1.46	2.01	2.54	2.91
PSNR of Restored Image (dB)	29.33	30.74	29.31	25.8	24.27
PSNR of Degraded Image (dB)	26.58	24.04	22.71	21.76	21.06
Computation Time (s)	319	349	383	395	432

Table 2 summarizes the experimental results: estimated blurred level, PSNR values of restoration images and degradation images, computation time for restoration. Fig.9, which indicates PSNR values of restoration images and degradation images, demonstrates the following result. Though the PSNR improvement is smaller in case of light blurring ($\sigma = 1.0$), PSNR of restoration image becomes almost 30dB due to its originally high PSNR of the blurred image. In case of typical blurring ($\sigma = 1.5-2.0$), the PSNR improvement becomes larger and also PSNR of restoration image becomes almost 30dB. In case of severe blurring ($\sigma = 2.5-3.0$), since it is not so easy to perform high quality restorations, PSNR of restoration image remains at almost 25dB. Briefly speaking, the

proposed restoration method can accomplish a high quality restoration (PSNR ≈ 30 dB) in case of $\sigma \leq 2.0$ and can maintain a stable restoration (PSNR ≈ 25 dB) in case of $\sigma \geq 2.5$. As mentioned above, since stable restorations are accomplished in both a visual inspection and PSNR evaluation, it can be confirmed that the proposed restoration method is practical and promising for various applications.

Furthermore, the computation time for the restoration is indicated in Fig.10. Note that the PC used in the experiments incorporates Intel Pentium-IV CPU (1.7 GHz). For each blurred level, the computation time can be reasonable since it takes 5-7 minutes approximately. The increase for the computation time with the increase of blurred level intensity will be caused by the increase of processing amount based on the degree extent of FIR filters.

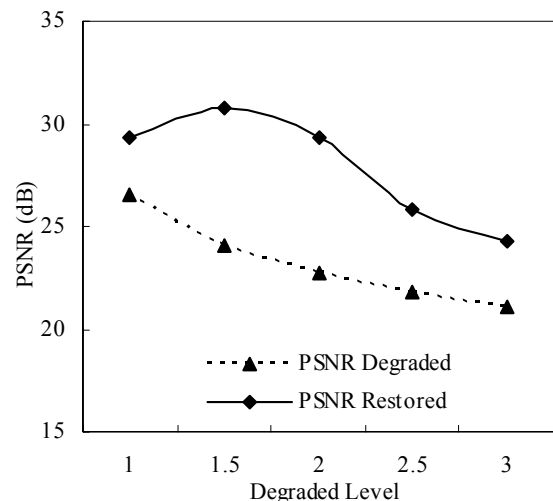


Fig.9 PSNR of restoration and degradation images

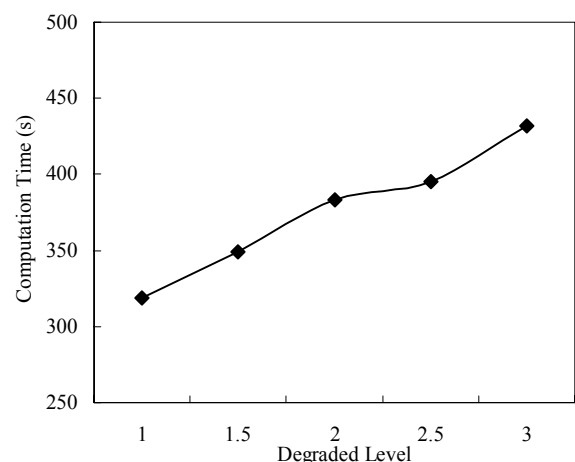


Fig.10 Computation time for restoration

6 Conclusion

In this paper, we have proposed a new restoration approach to blurred image using optimized inverse filter by a Rc-GA. Our proposed approach is characterized by an adaptive restoration according to its blurred level and a high-speed restoration based on efficient GA-search of inverse filters. Some experiments on natural images with out-of-focus blur demonstrate that, independent of features and blurred level of natural images, our proposed approach can restore blurred images with stability. We have confirmed that the proposed approach can provide a practical solution for a high-speed image restoration. In future, we will verify the validity of our proposed approach, in case of general degradation model including other type of blur and additive noise.

References:

- [1] A. Rosenfeld and A. C. Kak, *Digital picture processing*, Academic Press, Florida, pp.276-287, 1982.
- [2] M. Takagi and H. Shimoda, *Handbook for Image Analysis*, Tokyo University Publishing Association, pp. 383-422, 1995. (In Japanese)
- [3] M. R. Banham and A. K. Katsaggelos, *Digital Image Restoration*, IEEE Signal Processing Magazine, vol.14, no.2, pp. 24-41, 1997.
- [4] J. Holland, *Adaptation in Natural Artificial Systems*, the University of Michigan Press (Second Edition; MIT Press 1992).
- [5] K. Takatsu, H. Sawai, S. Watanabe, and M. Yoneyama, *Genetic Algorithms Applied to Bayesian Image Restoration*, IEICE Trans. Fundamentals, Vol.J77-D-II, No.9, pp. 1768-1777, 1994. (In Japanese)
- [6] T. Kurata, K. Mori, T. Fuchida, and T. Morishima, *Genetic Algorithms Applied to Bayesian Image Restoration*, IEICE Trans. Fundamentals, Vol.J81-D-II, No.9, pp. 2104-2111, 1998. (In Japanese)
- [7] H. Nishikado, H. Murata, M. Yamazi, and H. Yamauchi, *Blurred Image Restoration by Using Real-Coded Genetic Algorithm*, IEICE Trans. Fundamentals, Vol.E85-A, No.9, 2002. (In Japanese)
- [8] D. Kundur and D. Hatzinakos, *Blind Image De-convolution*, IEEE Signal Processing Magazine, vol.13, no.5, pp. 43-64, 1996.
- [9] I. Ono and S. Kobayashi, *Real-coded Genetic Algorithm for Function Optimization Using Unimodal*

Normal Distribution Crossover, Proc. of 7th Int. Conf. on Genetic Algorithms, pp.246-253, 1997.

[10] H. Kita, I. Ono, and S. Kobayashi, *Theoretical Analysis of the Unimodal Normal Distribution Crossover for Real-Coded Genetic Algorithms*, Proc. of 1998 IEEE Int. Conf. on Evolutionary Computation, 529-534, 1998.

[11] H. Urabe, *Development process, feature, and how to use Standard High Precision Picture data*, IIEEJ Journal, Vol.31, No.1, pp.110-115, 2002. (In Japanese)